

Construction of porous 2D MOF nanosheets for rapid and selective adsorption of cationic dyes

Huijie Li, Kuan Gao, Bingyan Mo, Qing Meng, Ke Li, Jie Wu,* and Hongwei Hou*

College of Chemistry, Zhengzhou University, Zhengzhou 450001, P. R. China.

Contents

Fig. S1 ^1H NMR spectrum of Zr-BTB.

Fig. S2 ^1H NMR spectrum of Zr-BTB- H_4TBAPy .

Fig. S3 ^1H NMR spectrum of PCN-134-2D.

Fig. S4 FTIR spectra of Zr-BTB, PCN-134-2D and Zr-BTB- H_4TBAPy nanosheets.

Fig. S5 (a) SEM image and (b-d) EDX mapping of Zr-BTB nanosheets.

Fig. S6 (a) SEM image and (b-e) EDX mapping of PCN-134-2D nanosheets.

Fig. S7 TEM images of Zr-BTB- H_4TBAPy at different sizes.

Fig. S8 (a) AFM image and (b) corresponding height profiles of Zr-BTB.

Fig. S9 The TGA diagrams of Zr-BTB, PCN-134-2D and Zr-BTB- H_4TBAPy .

Fig. S10 Chemical structures of various dyes employed.

Fig. S11 UV-vis spectra of (a) RhB (b) MLB (c) MB and (d) MO.

Fig. S12 Dye adsorption abilities to MB, MO, RhB and MLB as a function of time by (a) Zr-BTB- H_4TBAPy and (b) PCN-134-2D.

Fig. S13 (a) Adsorption abilities of different doses of Zr-BTB- H_4TBAPy to MB. (b) Adsorption abilities of Zr-BTB- H_4TBAPy to MB at varied temperature.

Fig. S14 Effects of contact time on the (a) RhB and (b) MLB adsorption of Zr-BTB- H_4TBAPy and PCN-134-2D.

Fig. S15 The UV-Vis spectra and adsorption images of MO and MLB mixed dye solutions before and after adsorption onto the Zr-BTB- H_4TBAPy .

Fig. S16 Recycle of the removal efficiency of Zr-BTB- H_4TBAPy for RhB.

Fig. S17 (a) The SEM image of the Zr-BTB- H_4TBAPy after 4 cycles. (b) The XRD patterns of before and after 4 cycles for Zr-BTB- H_4TBAPy .

Fig. S18 Zeta potential of Zr-BTB at pH=7.

Fig. S19 (a) Adsorption uptakes of MLB in the Zr-BTB-H₄TBAPy and PCN-134-2D nanosheets (b) Temkin, (c) Freundlich and (d) Langmuir isotherm models.

Table S1 Characteristic parameters of the adsorption of MLB on the Zr-BTB-H₄TBAPy and PCN-134-2D.

Table S2 Characteristic parameters of the adsorption of RhB on the Zr-BTB-H₄TBAPy and PCN-134-2D.

Synthesis of Zr-BTB

The 2D zirconium-based metal-organic frameworks (MOFs) Zr-BTB were prepared according to previous report. A mixture of $ZrCl_4$ (100 mg), H_3BTB (100 mg), benzoic acid (6g), water (5 mL) and DMF (30 mL) was introduced into a Pyrex vial. The mixture was heated in 120 °C oven for 48 h. After cooling down to room temperature, the obtained solid was collected by centrifugation, and washed several times with DMF and acetone. Then the product was dried at 60 °C under vacuum for 12 h, resulting in white Zr-BTB nanosheets.

Activation of Zr-BTB

Approximately as-synthesized Zr-2D-MOF sample (40 mg) was soaked in a mixture of DMF (12 mL) and 8 M aqueous HCl (0.5 mL) at 100 °C for 24 h to remove unreacted starting ligands, inorganic species and trapped benzoic acid. After cooling down to room temperature, the solution was removed and the residual was washed twice with DMF. Subsequently the solid residue was washed twice with acetone and soaked in acetone for additional 12 h. Zr-2D-MOF nanosheets were collected by centrifugation and activated at 60 °C under vacuum for 12 h.

Synthesis of PCN-134-2D

H_2TCPP (87 mg) in DMF (10 mL) was ultrasonically dissolved for 10 min in a 20 mL Pyrex vial. Then Zr-BTB nanosheet (50 mg) was added and incubated in the solution at 100 °C for 12 h. After cooling down to room temperature, the obtained solid powder was collected by centrifugation and washed several times with DMF and acetone. The product was dried at 60 °C under vacuum for 12 h, yielding light brown crystals. To determine TCPP/BTB ratio of PCN-134-2D, around 5 mg of samples were dissolved in 1 mL of a 10% $D_2SO_4/DMSO-d_6$. The TCPP/BTB ratio was determined to be 0.25 by 1H -NMR measurements.

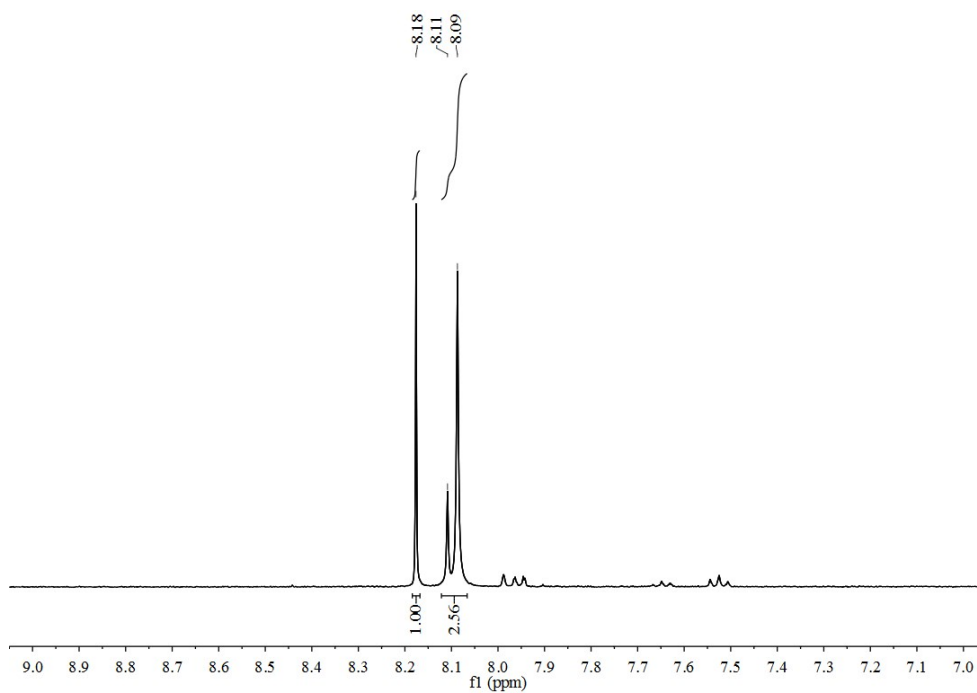


Fig. S1 ^1H NMR (400 MHz, DMSO- d_6) spectrum of Zr-BTB.

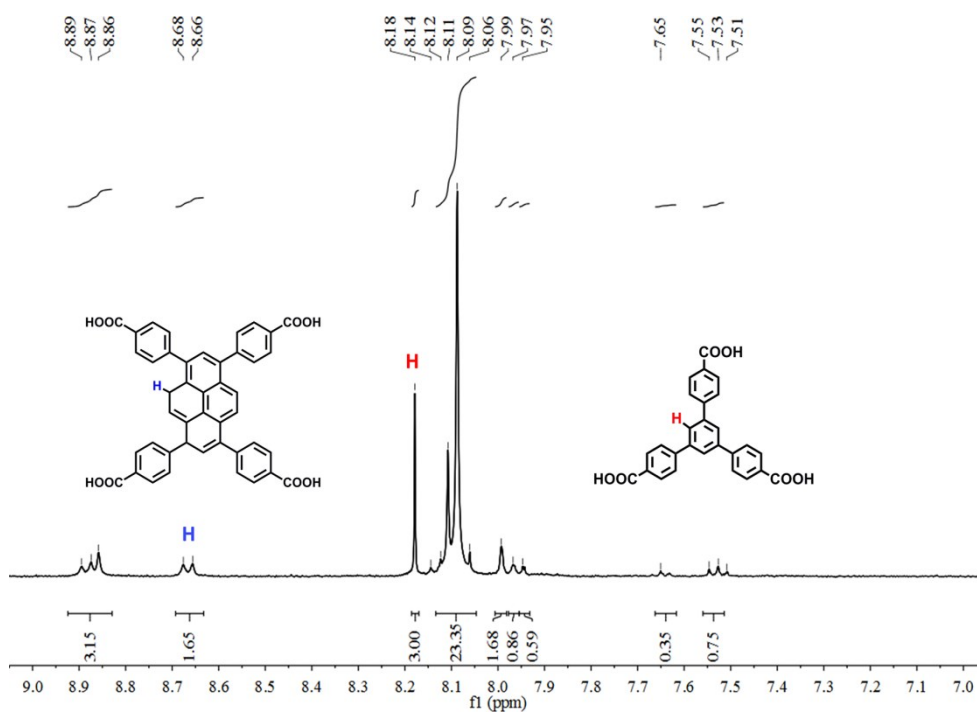


Fig. S2 ^1H NMR (400 MHz, DMSO- d_6) spectrum of Zr-BTB- H_4TBAPy .

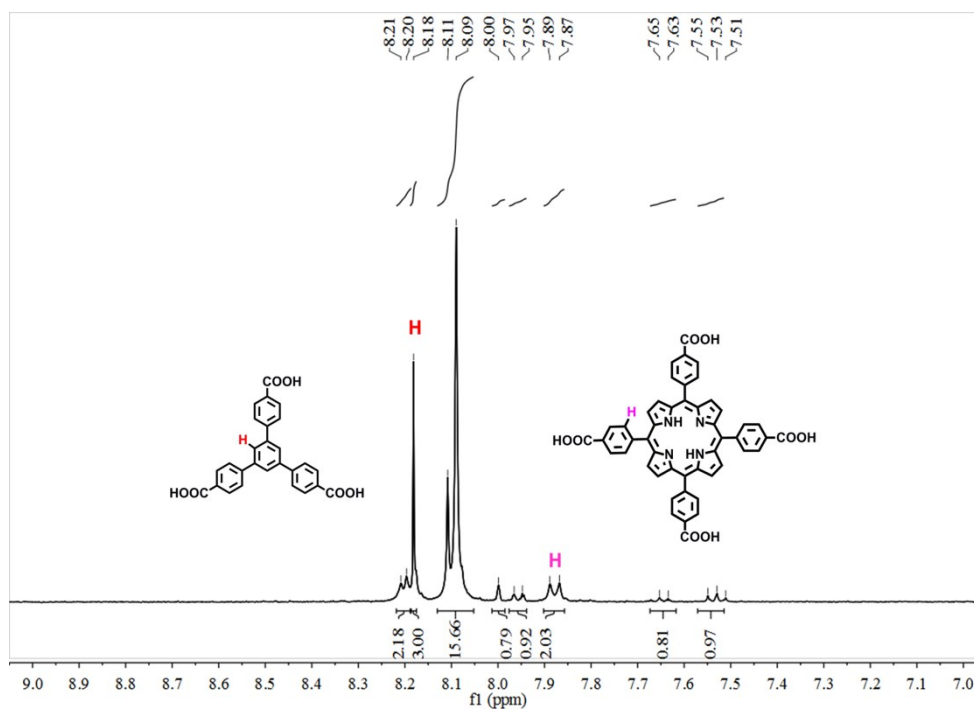


Fig. S3 ^1H NMR (400 MHz, DMSO- d_6) spectrum of PCN-134-2D.

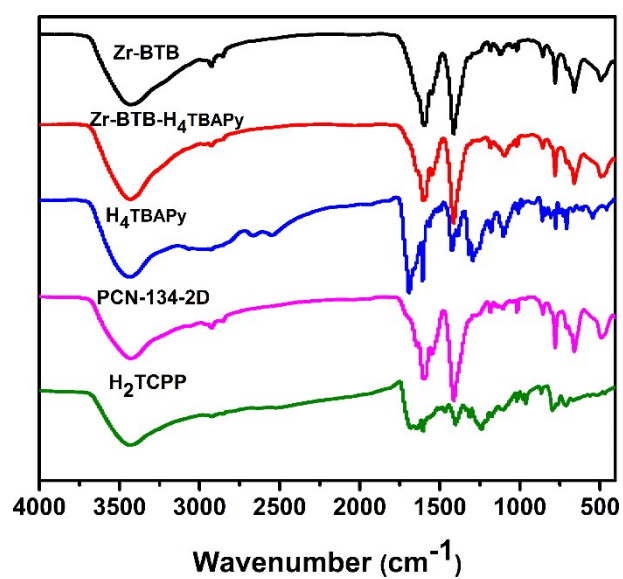


Fig. S4 FTIR spectra of Zr-BTB, PCN-134-2D and Zr-BTB- H_4TBAPy nanosheets.

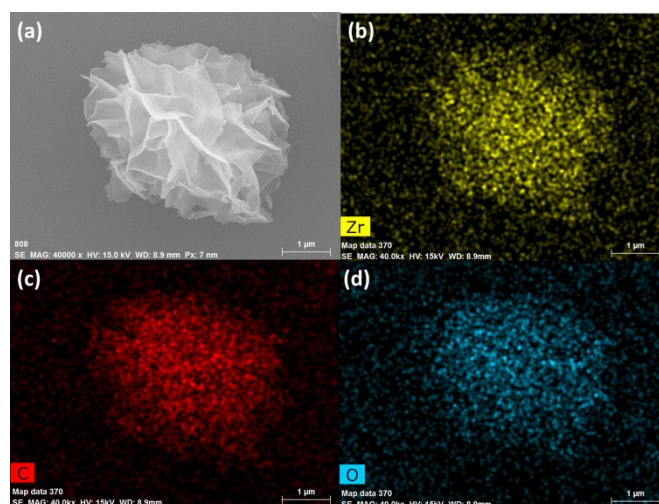


Fig. S5 (a) SEM image and (b-d) EDX mapping of Zr-BTB nanosheets.

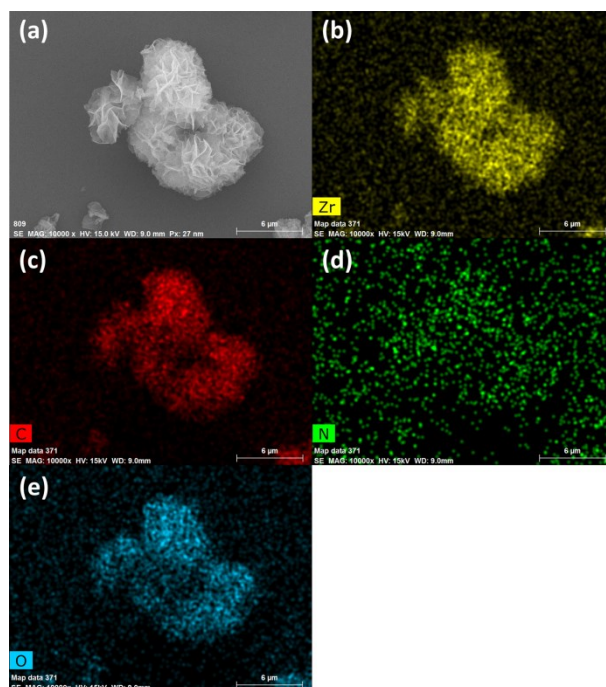


Fig. S6 (a) SEM image and (b-e) EDX mapping of PCN-134-2D nanosheets.

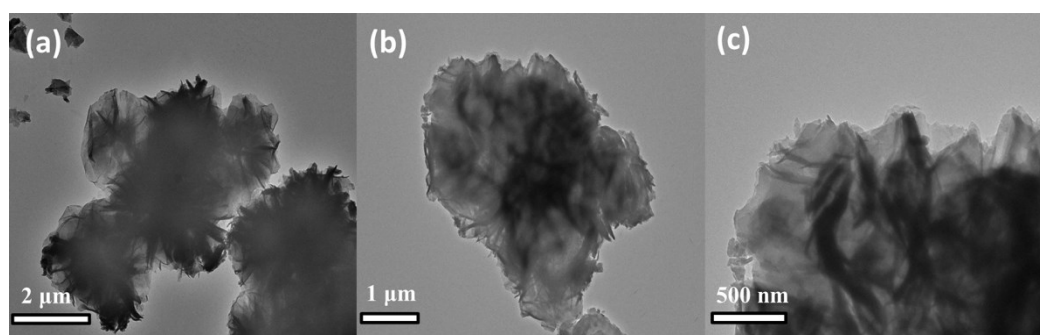


Fig. S7 TEM images of Zr-BTB-H₄TBAPy at different sizes.

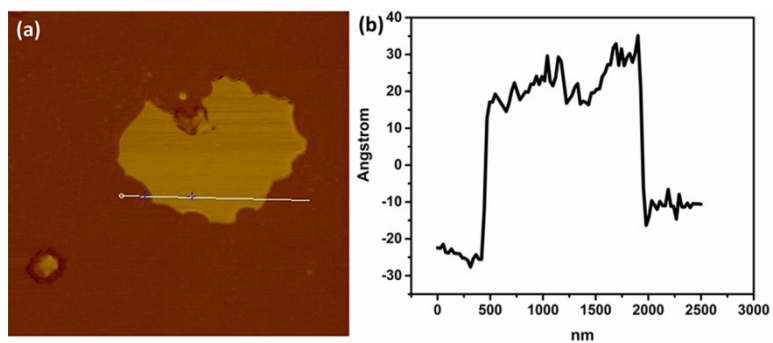


Fig. S8 (a) AFM image and (b) corresponding height profiles of Zr-BTB.

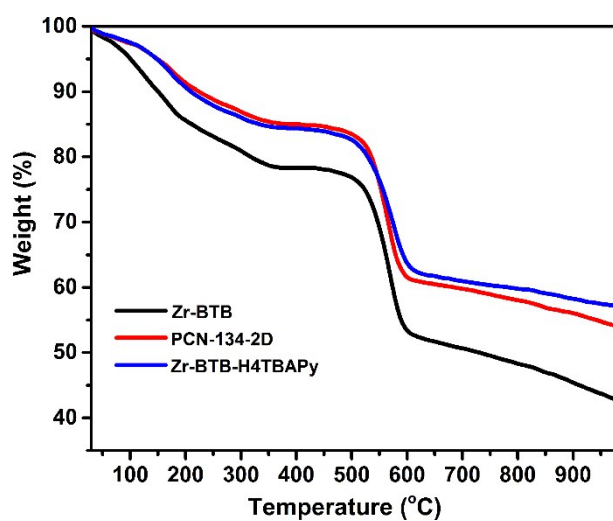


Fig. S9 The TGA diagrams of Zr-BTB, PCN-134-2D and Zr-BTB-H₄TBAPy under air condition.

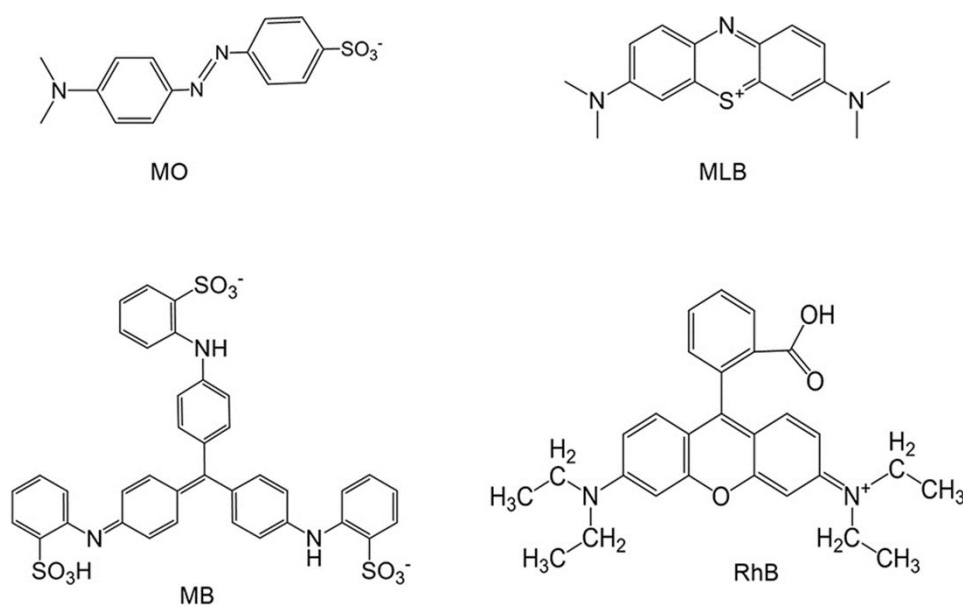


Fig. S10 Chemical structures of various dyes employed.

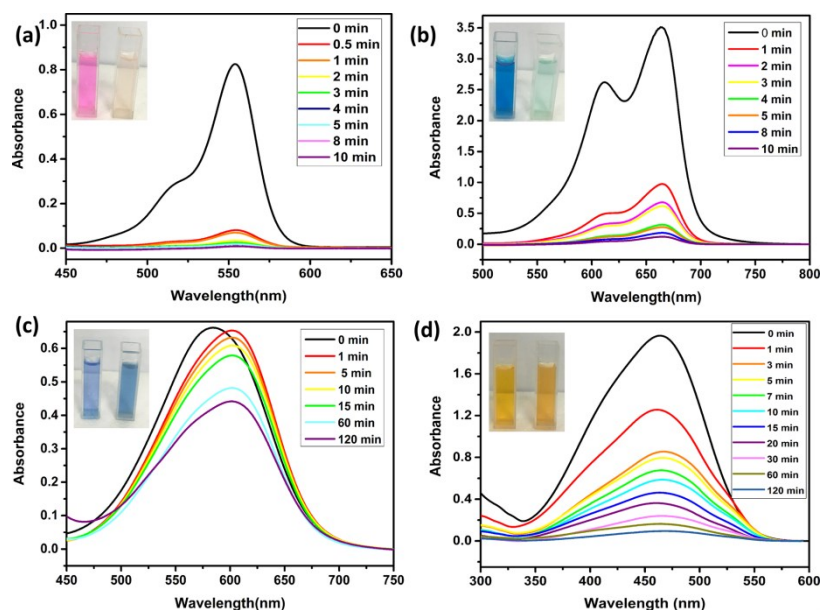


Fig. S11 UV-vis spectra of (a) RhB (b) MLB (c) MB (d) MO in aqueous solutions at different times during the adsorption experiments with PCN-134-2D as the adsorbent and the corresponding photographic images of adsorption during 10 min.

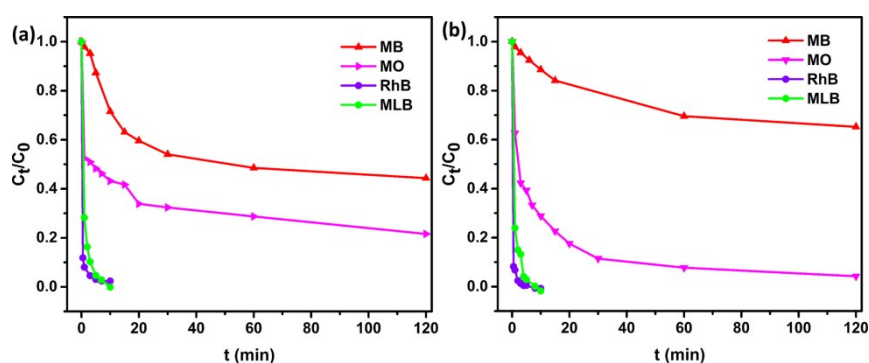


Fig.S12 Dye adsorption abilities to MB, MO, RhB and MLB as a function of time by (a) Zr-BTB-H₄TBAPy and (b) PCN-134-2D.

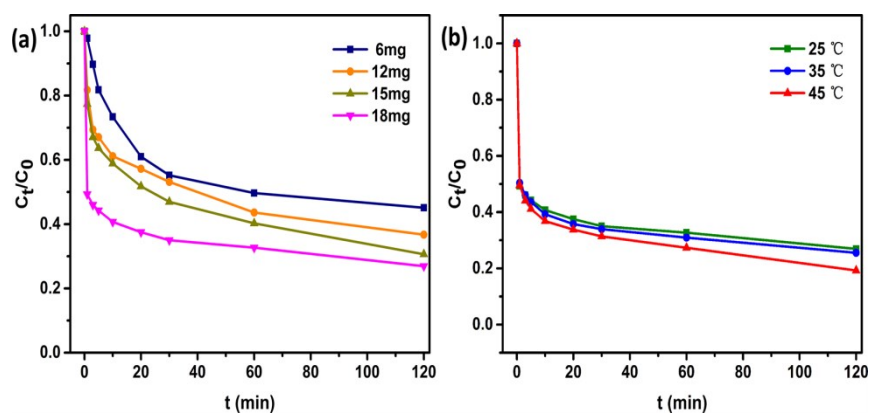


Fig. S13 (a) Adsorption abilities of different doses of Zr-BTB-H₄TBAPy to MB. (b) Adsorption abilities of Zr-BTB-H₄TBAPy to MB at varied temperature.

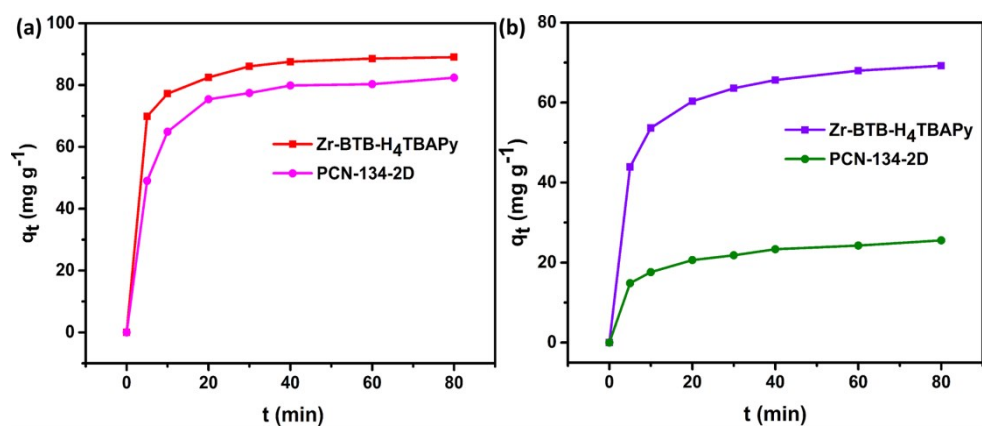


Fig. S14 Effects of contact time on the (a) RhB and (b) MLB adsorption of Zr-BTB- H_4 TBAPy and PCN-134-2D.

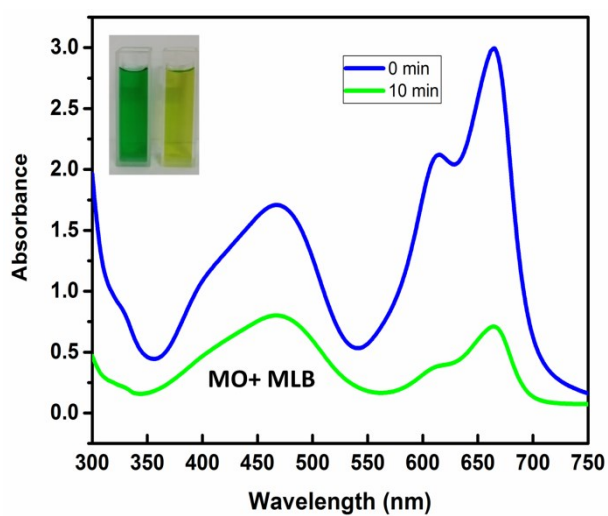


Fig. S15 The UV-Vis spectra and adsorption images of MO and MLB mixed dye solutions before and after adsorption onto the Zr-BTB- H_4 TBAPy.

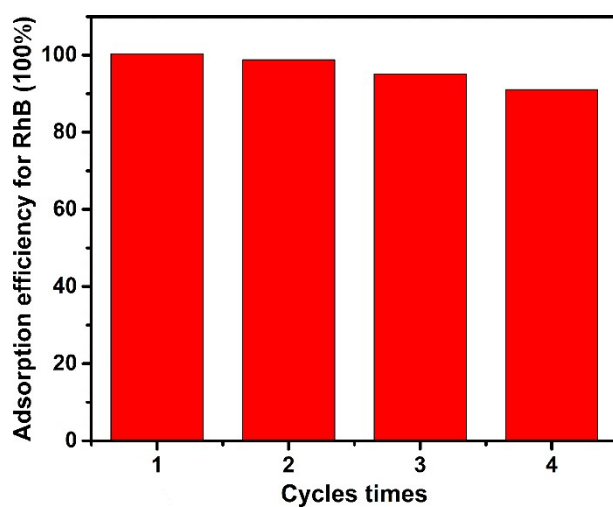


Fig. S16 Recycle of the removal efficiency of Zr-BTB- H_4 TBAPy nanosheet for RhB.

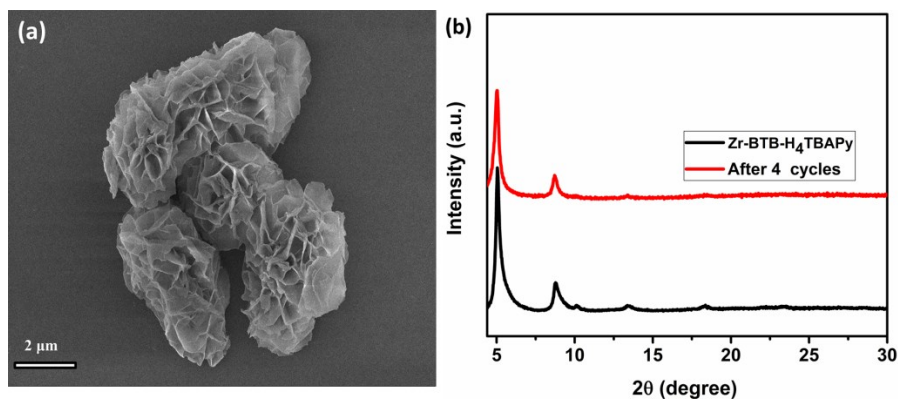


Fig. S17 (a) The SEM image of the Zr-BTB-H₄TBAPy after 4 cycles. (b) The XRD patterns of before and after 4 cycles for Zr-BTB-H₄TBAPy.

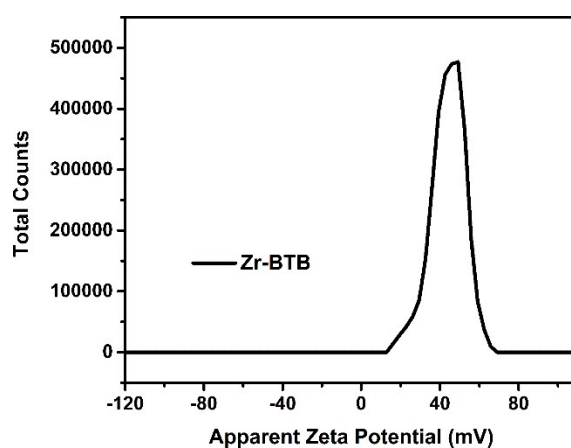


Fig. S18 Zeta potential of Zr-BTB at pH=7.

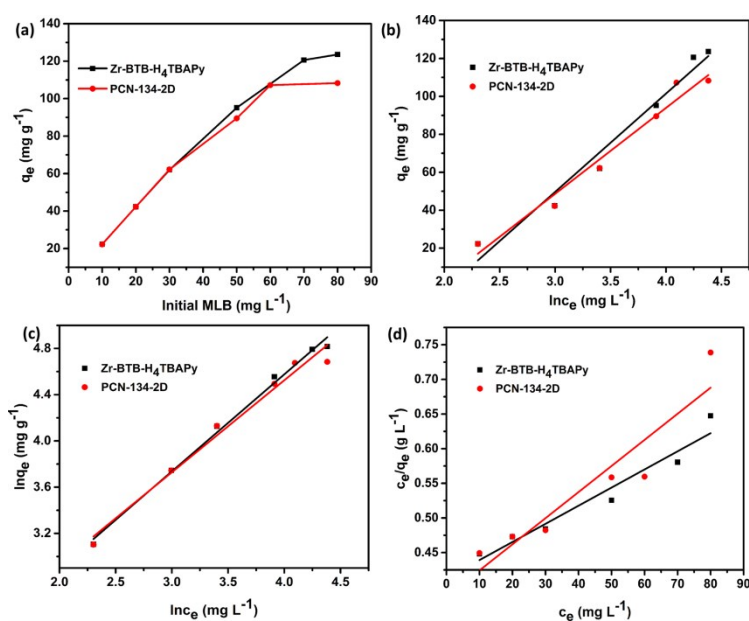


Fig. S19 (a) Adsorption uptakes of MLB in the Zr-BTB-H₄TBAPy and PCN-134-2D nanosheets after 24 h as a function of the initial MLB and plots of the fitting of the experimental data with (b) Temkin, (c) Freundlich and (d) Langmuir isotherm models.

Table S1 Characteristic parameters of the adsorption of MLB on the Zr-BTB-H₄TBAPy and PCN-134-2D.

		Shape	Zr-BTB-H ₄ TBAPy	PCN-134-2D
Adsorption kinetics	Pseudo-first-order	$q_{e,Exp}$ (mg g ⁻¹)	69.2	25.5
		$q_{e,Cal}$ (mg g ⁻¹)	28.4	11.6
		K_1 (min ⁻¹)	0.0527	0.0383
		R^2	0.991	0.981
	Pseudo-second-order	$q_{e,Exp}$ (mg g ⁻¹)	69.2	25.5
		$q_{e,Cal}$ (mg g ⁻¹)	72.1	26.9
		K_2 (g mg ⁻¹ min ⁻¹)	3.8×10^{-3}	6.7×10^{-3}
		R^2	0.999	0.998
Adsorption isotherm	Temkin	A (L g ⁻¹)	0.129	0.146
		B	51.7	45.3
		R^2	0.964	0.965
	Freundlich	n	1.19	1.26
		k_f (mg g ⁻¹ (Lmg ⁻¹) ^{1/n})	3.37	3.82
		R^2	0.992	0.974
	Langmuir	$q_{m,Exp}$ (mg g ⁻¹)	123.6	108.3
		$q_{m,Cal}$ (mg g ⁻¹)	381.7	265.3
		b (L mg ⁻¹)	6.34×10^{-3}	9.75×10^{-3}
R^2		0.938	0.851	
Thermodynamics		ΔG (kJ mol ⁻¹)	-3.01	-3.31

Table S2 Characteristic parameters of the adsorption of RhB on the Zr-BTB-H₄TBAPy and PCN-134-2D.

		Shape	Zr-BTB-H ₄ TBAPy	PCN-134-2D
Adsorption kinetics	Pseudo-first-order	$q_{e,Exp}$ (mg.g ⁻¹)	89.0	82.4
		$q_{e,Cal}$ (mg.g ⁻¹)	24.8	27.1
		K_1 (min ⁻¹)	0.0688	0.0498
		R^2	0.996	0.848
	Pseudo-second-order	$q_{e,Exp}$ (mg.g ⁻¹)	89.0	82.4
		$q_{e,Cal}$ (mg.g ⁻¹)	76.2	85.4
		K_2 (g mg ⁻¹ min ⁻¹)	6.1×10^{-3}	3.7×10^{-3}
		R^2	0.999	0.999
Adsorption isotherm	Temkin	A (L g ⁻¹)	0.0933	0.104
		B	78.4	67.9
		R^2	0.922	0.936
	Freundlich	n	1.19	1.27
		k_f (mg g ⁻¹ (L mg ⁻¹) ^{1/n})	3.23	3.03
		R^2	0.992	0.975
	Langmuir	$q_{m,Exp}$ (mg g ⁻¹)	238.4	203.2
		$q_{m,Cal}$ (mg g ⁻¹)	529.1	386.1
		b (L mg ⁻¹)	3.55×10^{-3}	6.67×10^{-3}
R^2		0.939	0.860	
Thermodynamics		ΔG (kJ mol ⁻¹)	-2.90	-2.75